

**STEP DECORATION AT Au SINGLE CRYSTAL ELECTRODES  
- IMPACT ON ADSORPTION AND CATALYSIS**

Fernando Hernandez<sup>(1)</sup>, Jean Sanabria-Chinchilla<sup>(1)(a)</sup>, Manuel P. Soriaga<sup>(2)</sup>, Helmut Baltruschat<sup>(1)\*</sup>

(1) University of Bonn, Roemerstrasse 164, D-53117 Bonn, Germany

(2) Electrochemical Surface Science Laboratory, Chemistry Department,  
Texas A&M University, USA

**ABSTRACT**

Surfaces of regularly stepped single crystals can be decorated with foreign metals in order to change their physicochemical properties. Step decoration of vicinally stepped platinum single crystals was achieved for many metals and can be easily monitored by cyclic voltammetry due to the suppression of the corresponding hydrogen adsorption at step sites. By using the system Pd/Au(hkl) reactive bonding sites are introduced at regular spacings. Here step decoration is more difficult to prove. Au(111) and Au(332) were used as the substrate for palladium deposition in the UPD-regime. Preparation and Pd deposition were checked by STM. Cyclic voltammetry shows two Pd-oxidation peaks, the first one being almost independent of coverage; it is therefore ascribed to Pd decorating steps. Hydrogen adsorption on the modified stepped surfaces, but not on Pd/Au(111), takes place only when more than a critical amount of Pd has been deposited. A voltammetric peak at ca. 0.3 V vs. RHE is related to the adsorption of hydrogen at palladium terraces, at this potential the adsorption of hydrogen on steps is negligible. A quantitative evaluation supports the assumption of step decoration by Pd. Using differential electrochemical mass spectrometry (DEMS), CO and benzene adsorbing at step sites was distinguished from that adsorbing at terraces.

**INTRODUCTION**

When studying bimetallic catalysts it is advantageous to use surfaces with an ordered arrangement of the two elements in order to get a fundamental insight into the manner of action of such systems. While for studies of the metal/gas interface often ordered bimetallic alloys are used, for studies at the metal/electrolyte interface such alloy systems require a UHV-transfer system in order to control the surface composition and order (1, 2). An alternative is the use of vicinally stepped single crystal electrodes, after step decoration with a second metal. In this way bimetallic metal surfaces are obtained, on which striped domains of the substrate alternate with monoatomic rows of the second component. In the case of stepped Pt single crystal

---

<sup>(a)</sup> On leave from: Electrochemical Surface Science Laboratory, Chemistry Dept., Texas A&M University, sanabria@mail.chem.tamu.edu

\* Corresponding author: baltruschat@uni-bonn.de

electrodes with (111) terraces, step decoration can be easily controlled by monitoring the suppression of the corresponding peaks in the cyclic voltammogram for hydrogen adsorption (3).

Decorating the steps of a Pt(332) electrode with Sn thus leads to a surface which is much more catalytically active for CO oxidation than a Pt(111) electrode modified by submonolayer amounts of Sn, because in the latter case Sn forms 2D islands after adsorption of CO, whereas on the (332) surface, due to step decoration, the Sn atoms are better and more homogeneously distributed (4-6). Up to 50% of the adsorbed CO is oxidizable at 0.3 V, the oxidation potential of the residual adsorbate is hardly shifted with respect to the pure Pt surface. Assuming that surface diffusion of CO is fast, a bifunctional effect of Sn on the CO oxidation on this surface can thus be excluded, because then all adsorbed CO should be oxidized at a lower potential. Instead, Sn exerts an electronic effect on CO and forces part of it into a weakly adsorbed state, which is more easily oxidized.

We have also demonstrated that decoration of steps with Ru is possible as well (7, 8). The oxidation of adsorbed CO at such a surface proceeds in only one oxidation peak (around 0.5 V as compared to 0.7 V on pure Pt), when the steps, and thus the rows of Ru, are not more separated than by a 5 atom wide terrace. When the distance between the rows of Ru is larger (e.g. 10 Pt atoms) a further oxidation peak is observed at 0.6 V. We concluded that this is due to CO adsorbed at some distance from the Ru, which is not subject to an electronic effect of Ru. The first oxidation peak, however, corresponds to CO adsorbed in close vicinity of Ru where it is subject to such an electronic effect (decreased adsorption enthalpy). The more positive oxidation peak is still located at a much lower potential than at pure Pt due to a bifunctional effect of Ru; assuming again fast diffusion of adsorbed CO to Ru sites, the activation barrier is decreased for both. In this way, also ternary surfaces can be prepared; further decoration of the Ru/Pt(332) system, e.g. with Mo, led to a surface which is catalytically more active than Ru/Pt(332) or Pt(332) (9).

Step decoration by catalytically inactive metals confirmed the importance of steps for hydrogenation reactions, as in the case of Cu/Pt(332) for hydrogenation of benzene (10). On the other hand, such a surface should also help in understanding geometric effects: Since the diameter of a benzene molecule corresponds to approx. 3 Pt atoms, its adsorption on a Pt(331) surface, with its only 2 atoms wide terraces might be largely suppressed after step decoration by Cu or Ag. However, the benzene coverage of ca.  $0.2 \text{ nmol cm}^{-2}$  as determined by DEMS in pure supporting electrolyte after adsorption at 0.3 V and electrolyte exchange, is similar to that of Pt(332) after step decoration by Cu or Ag, and only reduced by 50% with respect to the undecorated surface. Obviously, binding to only one row of accessible Pt atoms after step decoration is sufficient for strong, irreversible binding (11).

As an alternative to obtaining a bimetallic surface with alternating atoms of a catalytically active and inactive metal, Pd UPD-deposition on Au (332) is used in this work. Underpotential deposition of Pd on smooth Au(111) surfaces has been described by a number of authors (12-15).

## EXPERIMENTAL

Disc-shaped gold single crystals (Metal Crystals and Oxides LTD, 10 mm diam.) were prepared by flame annealing. After 2 minutes of annealing, they were transferred to the electrochemical cell and cooled down for 4 minutes over deaerated

Millipore water in a controlled atmosphere of either ultra pure argon (99.999%, Air Products) or in a reductive atmosphere of Ar:H<sub>2</sub> (2:1 vol.). After cooling, the quality of the surface was checked by cyclic voltammetry in 0.1 M H<sub>2</sub>SO<sub>4</sub> (Merck supra pur). All measurements were made at room temperature. In some experiments the surface quality was also controlled taking STM images. Examples are shown in fig. 1. It is clear from these images that cooling in Ar leads to faceting of stepped surfaces (similar to Pt, see (16)), whereas after cooling in the hydrogen containing atmosphere the step width is close to the nominal width. If the crystal is cooled in air, faceting is even more pronounced and the terrace width gets larger, an effect that is evident in older STM images (17).

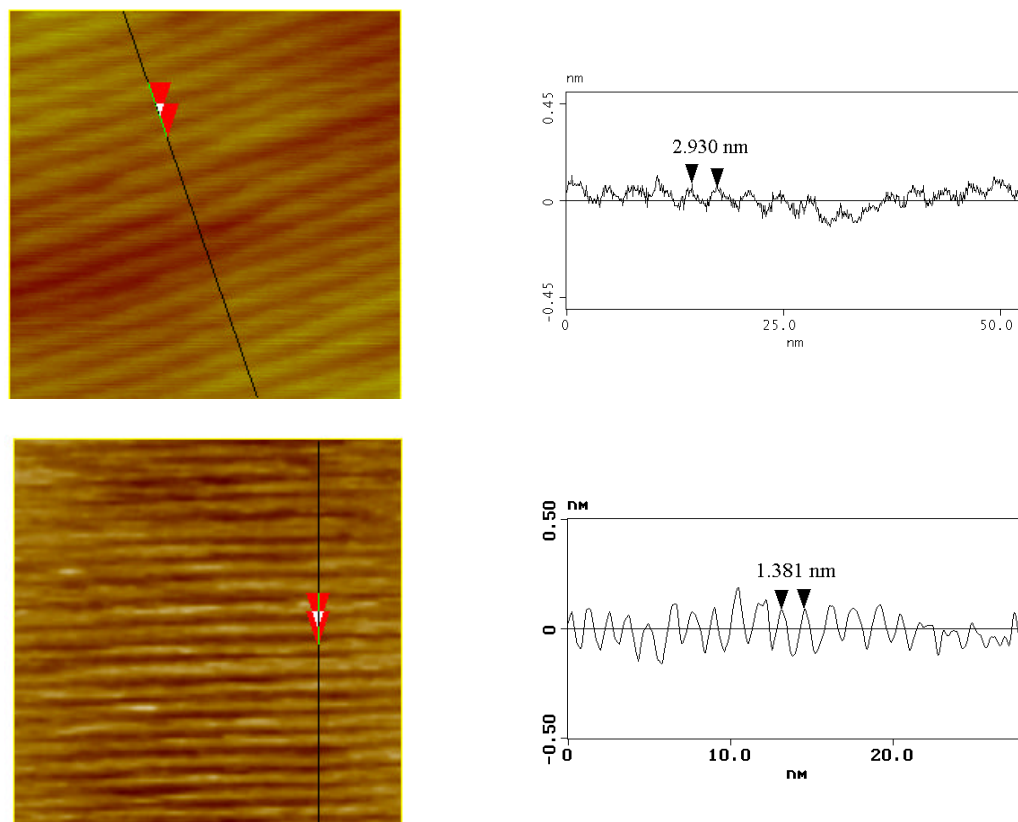


Fig. 1: STM-images of flame annealed Au(332). *Top*: 53 x 53 nm<sup>2</sup>, after cooling down in Ar. *Bottom*: 28 x 28 nm<sup>2</sup>, after cooling in Ar:H<sub>2</sub> atmosphere.

Millipore water was used to prepare all the solutions. A reversible hydrogen electrode (RHE) in 0.1 M H<sub>2</sub>SO<sub>4</sub> served as reference electrode for all the voltammetric experiments, while a Pt wire was used in the STM-cell as quasi reference electrode. The cyclic voltammograms were recorded in a glass cell in the hanging meniscus arrangement. Solutions were deaerated with ultra pure argon.

Two kinds of solutions were employed for the Pd deposition in the UPD-regime, namely one with chloride (0.1 mM PdCl<sub>2</sub> + 0.6 mM HCl + 0.1 M H<sub>2</sub>SO<sub>4</sub>) and one chloride-free (0.1 mM PdSO<sub>4</sub> + 0.1 M H<sub>2</sub>SO<sub>4</sub>). PdSO<sub>4</sub>·2H<sub>2</sub>O and PdCl<sub>2</sub> were obtained from Merck. The electrode was immersed at a potential of 1.16 V vs. RHE, where no Pd deposition takes place, and the potential was cycled slowly ( $v = 1$  mV/s) in the

cathodic direction until the UPD peak appeared. The charge under the UPD curve was used as a measure of the amount of Pd deposited, taking  $Q = 440 \mu\text{C cm}^{-2}$  as the equivalent charge for a full monolayer on the Au(111) surface. The integration was performed with the trapezoidal rule. To attain fractional coverage, the potential was stopped at a given value before the UPD peak was complete, breaking immediately the contact with the electrolyte and rinsing the electrode with water. This method was found to give more reproducible results than the selective dissolution of a previously deposited full Pd monolayer.

At the end of any experiment involving Pd deposition, the electrode was cycled in a solution containing 0.1 M  $\text{H}_2\text{SO}_4$  and 0.6 mM HCl at 50 mV/s between 0 and 1.7 V until a steady response was attained, changing the electrolyte several times if necessary. This procedure proved to be enough to dissolve all the deposited Pd, leaving a clean gold single crystal that can be annealed and used again. Details of differential electrochemical mass spectrometry (DEMS) are described elsewhere (18).

CO adsorption was performed for 3 min under potential control (0.35 V) using a CO-saturated 0.1 M  $\text{H}_2\text{SO}_4$  solution. After adsorption, the cell was rinsed with supporting electrolyte at the same adsorption potential. Scan was started cathodically to check the suppression of the H ads/des signals between 0.30 V and 0.10 V. After that, the positive switching potential was extended to 1.30 V.

## RESULTS AND DISCUSSION

Fig. 2 summarises the cyclic voltammetry for Au(332) covered by varying amounts of Pd. The pair of peaks at around 0.3 V corresponds to hydrogen adsorption and to some extent to anion desorption. The anodic peak at 0.9 V is independent of the Pd coverage whereas that above 1.0 V strongly depends on the Pd coverage. We, therefore, conclude that the latter is due to oxygen adsorption on Pd (UPD) terraces (and subsequent Pd dissolution) whereas the former is due to oxygen adsorption at steps. Its independence on the Pd coverage signifies that Pd decorates the steps indeed. If Pd islands on the Au terraces would form, their total edge length certainly would vary with Pd coverage. The Pd/Au(111) surface only shows the second peak. A further hint for step decoration is the height of the peak at 0.3V: at a coverage of 47% its height is only 1/3 of that of full Pd coverage. A plot of the peak current vs. coverage and extrapolation to zero peak height shows that hydrogen adsorption becomes appreciable only above a coverage of around 20%, which just corresponds to a decoration of the step edges with one row of Pd atoms.

Hydrogen adsorption on Au electrodes is usually not believed to occur. Recent theoretical calculations have shown that the adsorption energy of hydrogen on Au is much lower than that of Pd (19). On the other hand, hydrogen evolution observed during formaldehyde oxidation in alkaline solution on Au, Ag and Cu electrodes is known to occur via adsorbed hydrogen (20). Adsorbed hydrogen on Ag is formed during the injection of hot electrons in MIM structures (21). Recently, Stimming and co-workers interpreted their results on hydrogen evolution at Pd clusters generated from an STM tip by a spillover of hydrogen atoms onto the Au surface and their subsequent recombination on Au (22). Therefore, we have also studied the hydrogen evolution at the Pd decorating the steps of Au(332). The results are summarised in fig. 3, which gives the current - voltage curves in a hydrogen-saturated sulphuric acid solution at small overpotentials. Whereas at pure Au the exchange current density is negligible, at surfaces covered by submonolayers of Pd it is more than twice that of

the exchange current measured at a surface covered by nearly 2 monolayers. Interestingly, the current density hardly depends on the Pd coverage as long as it is below one monolayer. At all surfaces, the scan rate had no influence.

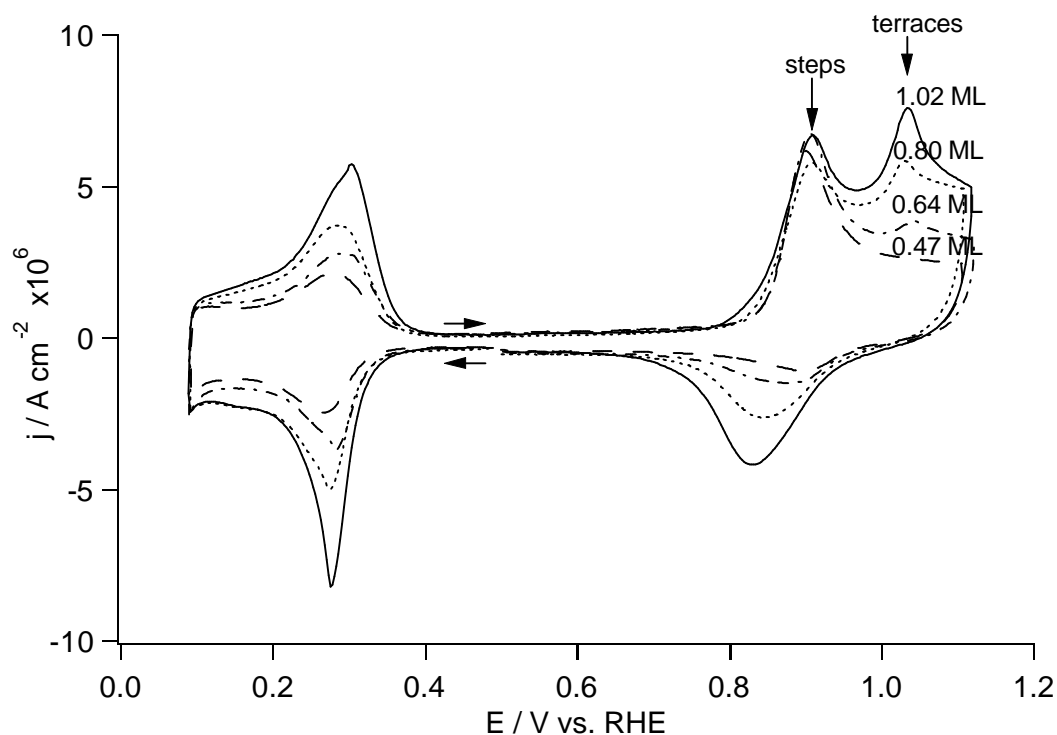


Fig. 2: First voltammetric cycle for Pd/Au(332) in 0.1 M H<sub>2</sub>SO<sub>4</sub> with different Pd coverage. Starting potential 0.5 V, scan rate of 5 mV/s. Pd was deposited from PdSO<sub>4</sub> solution.

A higher catalytic activity of UPD Pd as compared to that of bulk Pd has already been found by Kibler et al. and has been explained by the shift of the d-band centre. For submonolayers of Pd on Au(111) Stimming and co-workers have found that the exchange current density is not proportional to the coverage of Pd on Au(111); when normalised to the Pd coverage it decreases. This was interpreted by the spillover of hydrogen atoms from Pd to the uncovered Au surface, where formation of H<sub>2</sub> takes place more efficiently. This spillover of hydrogen atoms had already been suggested to explain the large catalytic activity of Pd nanoclusters on Au (22).

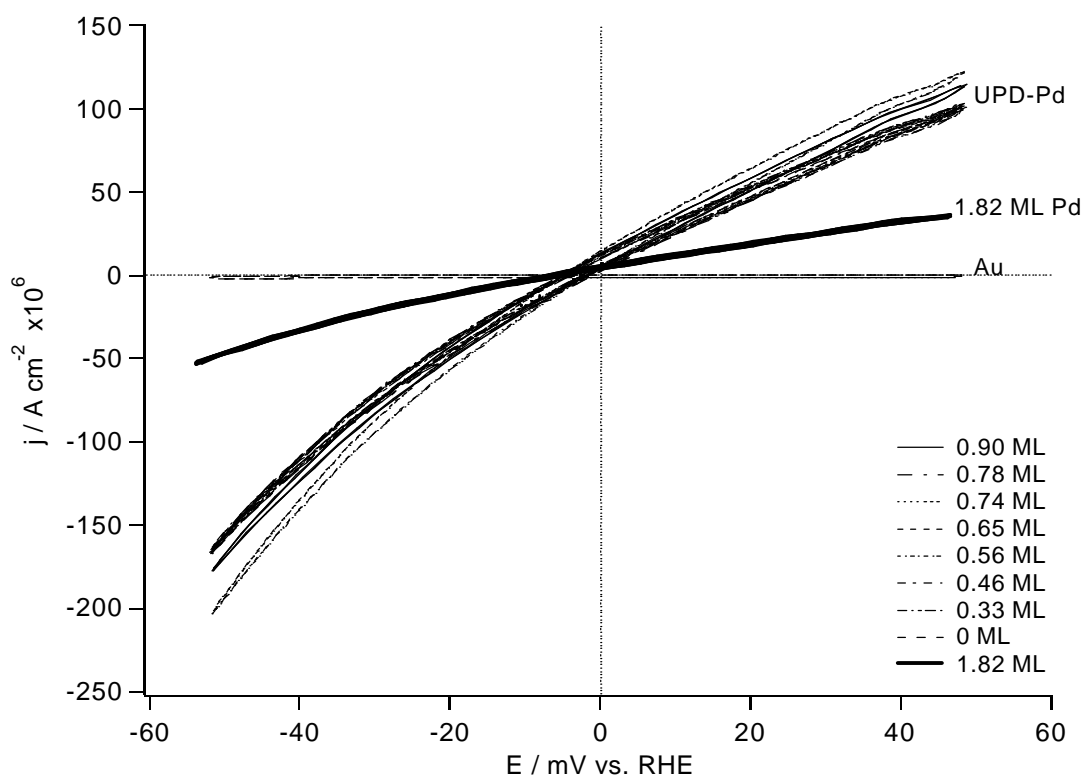


Fig. 3:  $\text{H}_2$ -evolution on Pd/Au(332) as a function of Pd-coverage. Current-voltage curves in 0.1 M  $\text{H}_2\text{SO}_4$  saturated with  $\text{H}_2$ , 25 mV/s (no effect of scan rate was found).

The independence of the reaction rate on coverage suggests that the rate of hydrogen evolution is proportional to the total step length. Assuming step decoration, this length does not vary with increasing Pd coverage on a stepped Au surface, whereas it does vary with coverage on Au(111) surfaces due to a changing number and size of Pd islands. Note that the step length is identical to the length of the boundary between Pd and Au as long as the coverage is below one monolayer. Therefore, this effect may be due to a particular catalytic activity of Pd steps, or to the importance of the Pd-Au boundary, which, assuming the hydrogen spillover to Au to be true, would limit the overall rate.

The decrease of the catalytic activity after deposition of a second monolayer probably has to be explained by an electronic effect. However, a change of the morphology also has to be considered. In fig. 4, the STM images during deposition of a second monolayer are shown. The result is a faceted surface; terraces become broader, but they are not continuous in step direction. This has to be compared to overpotential deposition of Pd on Au(111) which occurs in a layer-by-layer growth mode, however, the thicker the Pd layer, the less continuous the Pd layers are (12, 13, 15, 23, 24).

Oxidation of adsorbed carbon monoxide also demonstrates step decoration by Pd (fig 5). Differential electrochemical mass spectrometry (DEMS) was used here in order to distinguish the oxidation currents from (pseudo-) capacitive currents. On a surface covered by 0.78 monolayer of Pd, a peak at 0.93 V and a shoulder at 1.1 V are visible. When essentially only the steps are decorated by Pd (approx. 0.34 monolayers) only an oxidation peak at 1.1 V is visible, coinciding with the shoulder observed for the higher Pd coverage. This latter peak corresponds, therefore, to CO adsorbed either at Pd step sites or to sites in the direct vicinity of Au (steps of the

substrate). Since it is improbable that the neighbourhood to Au increases the adsorption strength, we favour the interpretation that the more anodic peak corresponds to CO adsorbed at step sites. Nevertheless, the oxidation may proceed at step sites also from molecules adsorbed at terrace sites, i.e. oxidation may well start at steps. But CO molecules diffuse from terrace sites to the steps and quickly refill those sites.

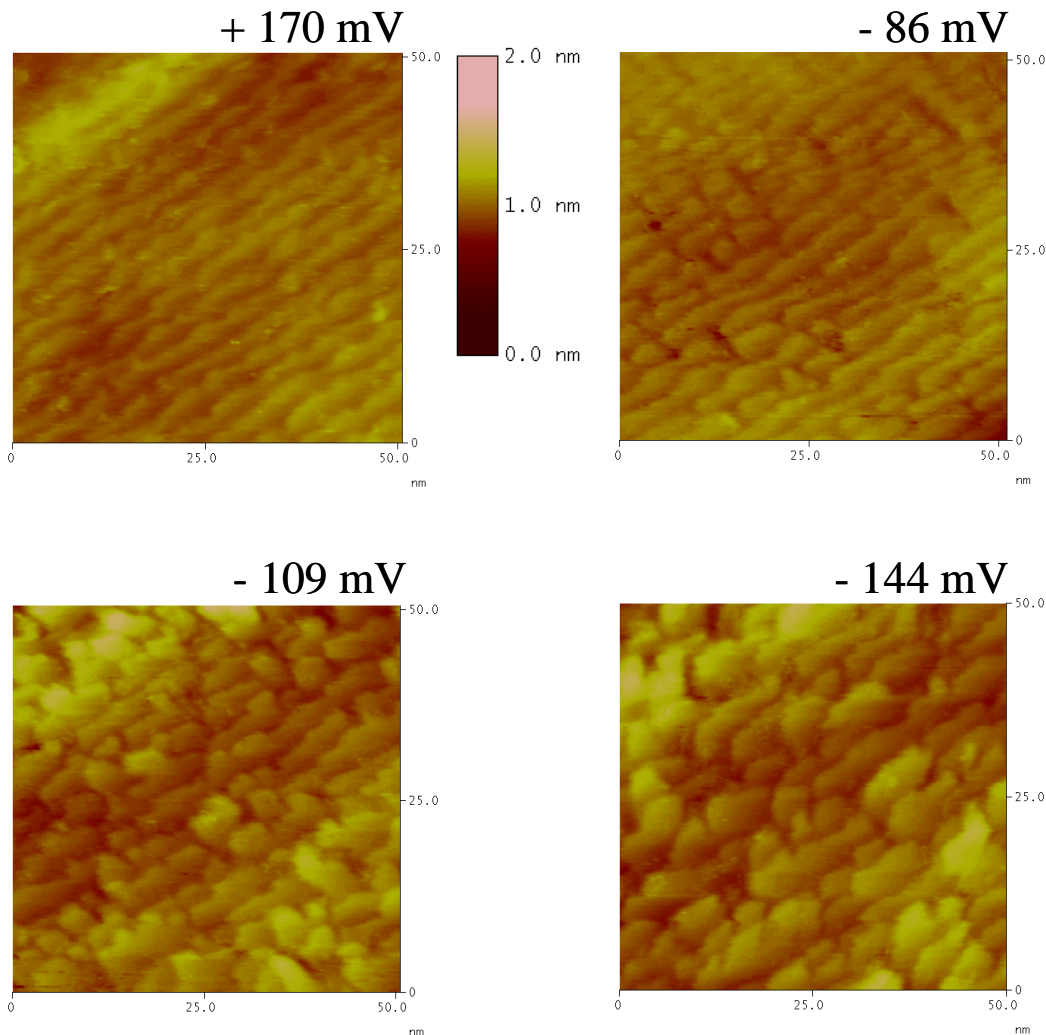


Fig. 4: Sequence of STM-images for Pd deposition from PdSO<sub>4</sub> solution on Au(332). *Top left:* original surface; *Top right:* 1<sup>st</sup>. Pd layer is complete. *Bottom:* Growth of subsequent layer. All potentials vs. Pt QRE. Area is 50 x 50 nm<sup>2</sup>.

Desorption of irreversibly adsorbed benzene on a Pd-modified Au(332) surface is monitored by the DEMS experiment shown in fig 6. From a surface fully covered by Pd, part of the adsorbate is desorbed during a potential sweep in the negative direction without hydrogenation. Some residual benzene is displaced by adsorbing oxygen in the subsequent anodic potential sweep. Qualitatively, a similar behaviour had been observed for benzene adsorbed on polycrystalline Pd (25). When only the steps are decorated by Pd, no benzene is desorbed at low potentials, but only in the oxygen adsorption region. Oxidation to CO<sub>2</sub> is negligible in both cases. The obvious interpretation is that benzene adsorbed at step sites is strongly adsorbed and is only displaced by oxygen, whereas benzene at terraces is desorbable at low potentials. Table 1 summarizes the results including the Au(111) face. Note that from an

Au(111) electrode largely covered by Pd, nearly all of the benzene desorbs at low potentials.

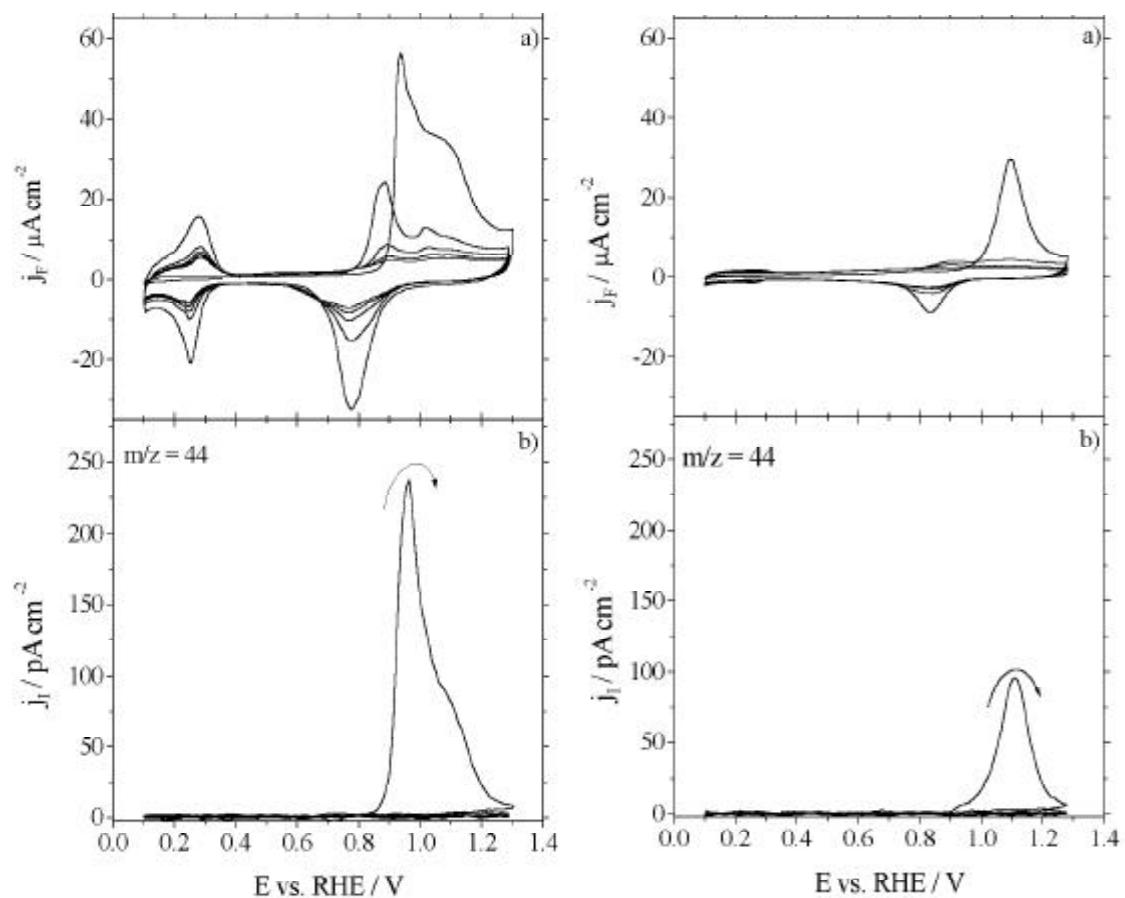


Fig. 5: CO oxidation on Pd/Au(332) surfaces. *a*) Cyclic voltammogram (CV) after CO adsorption, *b*) mass spectrometric cyclic voltammogram (MSCV) for  $m/z = 44$ , corresponding to  $\text{CO}_2$ .  $E_{\text{ad}} = 0.35 \text{ V}$ ,  $v = 10 \text{ mV/s}$ ,  $0.10 \text{ M H}_2\text{SO}_4$ . *Left*: 0.78 ML Pd, *right*: 0.34 ML Pd.

Table 1:

Summary of DEMS results for benzene desorption on Pd/Au(332) and Pd/Au(111).

Surface	$G_{\text{benzene}} / \text{nmol cm}^{-2}$	
	Hydrogen region	Oxide region
<b>0.94 ML Pd/Au(332)</b>	113.4	74.1
<b>0.16 ML Pd/Au(332)</b>	15.6	79.5
<b>0.60 ML Pd/Au(111)</b>	161.8	12.7



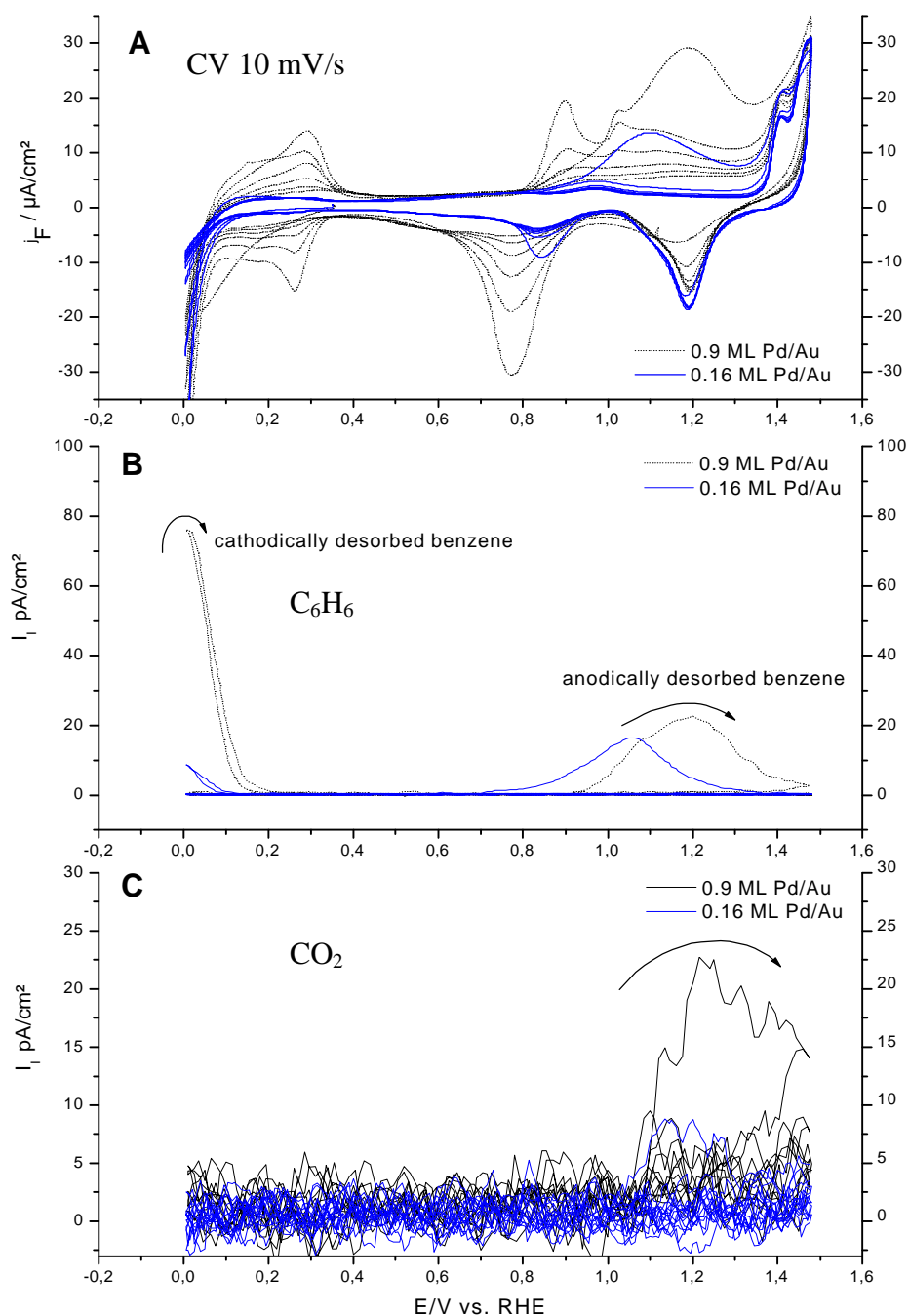


Fig. 6: Desorption of benzene on Pd/Au(332) surfaces. *a*) Cyclic voltammogram (CV) after benzene adsorption, *b*) mass spectrometric cyclic voltammogram (MSCV) for  $m/z = 78$ , benzene and *c*) MSCV for  $m/z = 44$ ,  $\text{CO}_2$ . Two different Pd coverages are shown.

#### ACKNOWLEDGEMENTS

This project would have not been possible without the support of the Deutsche Forschungsgemeinschaft (DFG). Fernando Hernandez and Jean Sanabria-Chinchilla thank the German Academic Exchange Service (DAAD) for their research grants.

#### REFERENCES

- (1) Hayden, B. E.; Rendall, M. E.; South, O. *J. Am. Chem. Soc.* **2003**, *125*, 7738-7742.

- (2) Stamenkovic, V. R.; M., A.; C.A., L.; Gallagher, M. E.; Ross, P. N.; Markovic, N. M. *J. Am. Chem. Soc.* **2003**, *125*, 2736-2745.
- (3) Clavilier, J.; Feliu, J. M.; Aldaz, A. *J. Electroanal. Chem.* **1988**, *243*, 419-433.
- (4) Massong, H.; Tillmann, S.; Langkau, T.; Abd El Meguid, E. A.; Baltruschat, H. *Electrochim. Acta* **1998**, *44*, 1379-1388.
- (5) Berenz, P.; Tillmann, S.; Massong, H.; Baltruschat, H. *Electrochim. Acta* **1998**, *43*, 3035-3043.
- (6) Tillmann, S.; Samjeske, G.; Friedrich, A.; Baltruschat, H. *Electrochim. Acta* **2003**, *49*, 73-83.
- (7) Massong, H.; Wang, H. S.; Samjeske, G.; Baltruschat, H. *Electrochim. Acta* **2000**, *46*, 701-707.
- (8) Samjeske, G.; Xiao, X.-Y.; Baltruschat, H. *Langmuir* **2002**, *18*, 4659-4666.
- (9) Samjeské, G.; Wang, H.; Löffler, T.; Baltruschat, H. *Electrochim. Acta* **2002**, *47*, 3681 - 3692.
- (10) Löffler, T.; Bussar, R.; Drbalkova, E.; Janderka, P.; Baltruschat, H. *Electrochim. Acta* **2003**, *48*, 3829 - 3839.
- (11) BuBar, R. Diploma thesis, University of Bonn, Bonn, 2002.
- (12) Naohara, H.; Ye, S.; Uosaki, K. *Colloid Surf. A-Physicochem. Eng. Asp.* **1999**, *154*, 201-208.
- (13) Takahasi, M.; Hayashi, Y.; Mizuki, J.; Tamura, K.; Kondo, T.; Naohara, H.; Uosaki, K. *Surface Sci.* **2000**, 213-218.
- (14) Baldauf, M.; Kolb, D. M. *Electrochim. Acta* **1993**, *38*, 2145-2153.
- (15) Kibler, L. A.; Kleinert, M.; Randler, R.; Kolb, D. M. *Surface Sci.* **1999**, *443*, 19-30.
- (16) Herrero, E.; Orts, J. M.; Aldaz, A.; Feliu, J. M. *Surface Sci.* **1999**, *440*, 259-270.
- (17) Adzic, R. R.; Hsiao, M. W.; Yeager, E. B. *Surface Science Letters* **1992**, *273*, L425-L429.
- (18) Baltruschat, H. In *Interfacial Electrochemistry*; Wieckowski, A., Ed.; Marcel Dekker, Inc.: New York, Basel, 1999, pp 577 - 597.
- (19) Roudgar, A.; Groß, A. *J. Electroanal. Chem.* **2003**, *548*, 121-130.
- (20) Stadler, R.; Z., J.; Baltruschat, H. *Electrochim. Acta* **2002**, *47*, 4485-4500.
- (21) Diesing, D.; Rübe, S.; Otto, A.; Lohrengel, M. M. *Ber. Bunsenges. Chem.* **1995**, *99*, 1402-1405.
- (22) Meier, J.; Schiotz, J.; Liu, P.; Norskov, J. K.; Stimming, U. *Chem. Phys. Lett.* **2004**, *390*, 440-444.
- (23) Naohara, H.; Ye, S.; Uosaki, K. *J. Phys. Chem. B* **1998**, *102*, 4366-4373.
- (24) Quayum, M. E.; Ye, S.; Uosaki, K. *J. Electroanal. Chem.* **2002**, *520*, 126-132.
- (25) Schmiemann, U.; Jusys, Z.; Baltruschat, H. *Electrochim. Acta* **1994**, *39*, 561-576.